INTERNATIONAL JOURNAL OF ENERGY STUDIES

e-ISSN: 2717-7513 (ONLINE); homepage: https://dergipark.org.tr/en/pub/ijes

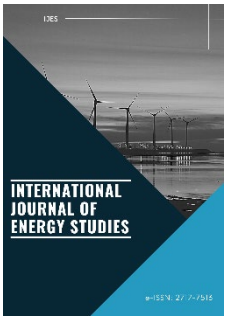

Research Article
Int J Energy Studies 2024; 9(4): 905-924
DOI: 10.58559/ijes.1530964

Received : 09 Aug 2024
Revised : 13 Oct 2024
Accepted : 25 Oct 2024

Design and simulation of a standing wave thermoacoustic refrigerator using air as the working fluid

Netice Duman[a*], Halil İbrahim Acar[b], Lutuf Ertürk[c]

[a]Sivas Cumhuriyet University Technical Sciences Vocational School, Sivas, Türkiye, ORCID: 0000-0002-9926-8511

[b]Sivas Cumhuriyet University, Faculty of Engineering, Department of Mechanical Engineering, Sivas, Türkiye, ORCID: 0000-0003-3951-6138

[c]Sivas Cumhuriyet University, Faculty of Engineering, Department of Mechanical Engineering, Sivas, Türkiye, ORCID: 0000-0002-2591-9094

*(*Corresponding Author:nduman@cumhuriyet.edu.tr)*

Highlights

- Thermoacoustic refrigerator (TAR) is one of the best technologies accepted as an alternative to traditional cooling systems.
- The theoretical design was made using the MATLAB program, and the validity of the obtained design values was investigated by entering them into the DeltaEC.
- The theoretical design and DeltaEC results are compatible with each other.
- Theoretical results show a better performance than DeltaEC results.

You can cite this article as: Duman N, Acar Hİ, Ertürk L. Design and simulation of a standing wave thermoacoustic refrigerator using air as the working fluid. Int J Energy Studies 2024; 9(4): 905-924.

ABSTRACT

Thermoacoustic refrigerator (TAR) is one of the best technologies accepted as an alternative to traditional cooling systems. Factors such as the fact that TAR systems have minimum environmental and human health problems such as global warming and ozone layer depletion, being lightweight and having no moving parts make these systems seen as promising clean technologies in the future. TAR creates a cooling effect by converting acoustic energy into thermal energy. In this research, a quarter wave standing wave thermoacoustic refrigerator using air as the working fluid and a speaker as an acoustic power source was designed and simulated. An algorithm suitable for the literature on thermoacoustics was used in the design. Simplified linear theory was used in this algorithm and the designed standing wave TAR model was simulated with the Design Environment for Low Amplitude Thermo Acoustic Energy Conversion (DeltaEC) program. In the study, the changes of various parameters along the resonator length were examined and the results were given graphically. Design and simulation cooling coefficient of performance (COP) results were 2.236 and 1.036 respectively.

Keywords: Thermoacoustics, Stack, Resonator, DeltaEC, Cooling coefficient of performance

1. INTRODUCTION

Thermoacoustics is the science that studies the conversion of heat energy into sound energy and sound energy into heat energy. While devices that convert heat energy into sound or acoustic work are generally called "heat engines", devices that take heat from a low-temperature source and transfer it to a high-temperature source using sound or acoustic work are called "thermoacoustic refrigerators". Although the thermoacoustic effect has been a known issue for a long time, rapid developments have been experienced in this field only in recent years. These developments have enabled the development of prototype devices based on thermoacoustic technology and a better understanding of the theoretical foundations. Thermoacoustic cooling stands out as a new cooling technology. Although this technology has advantages such as being promising, environmentally friendly and simple compared to vapor compression refrigerators, it also has the disadvantage that the cooling efficiency coefficients (COP) are not at the desired level [1-3].

The term thermoacoustics was first used by Sondhauss in 1850 and entered the scientific literature. Later, this phenomenon was called the "thermoacoustic effect" by Rayleigh (1878 and 1945). Rott et. al. derived the equations that formed the basis of thermoacoustic theory from 1969 to 1980 and presented the solutions of these equations in their articles [4,5].

The linear thermoacoustic theory introduced by Rott et al. was later developed by Swift and made widely applicable to study the acoustic properties and processes of thermoacoustic devices for low pressure amplitudes [6,7]. Since the pioneering work of Wheatley et al [8] in the early 1980s, there have been significant advances in the field of thermoacoustic research. The first successful thermoacoustic cooling device, released by Hofler [9] and having a cooling power of 6 W, is a result of these developments [4]. Additionally, many researchers such as Minner et al. [10], Reid and Swift [11], Tijani et al. [12], Hariharan et al [13] have conducted studies on the cooling effect that occurs as a result of the contact of the working fluid with solid surfaces.

Wetzel and Herman [14] developed a design algorithm that can be used as a simple design guide for thermoacoustic refrigerators. Tijani et al. [12] used this algorithm to design and build a thermoacoustic refrigerator. Many studies have been conducted by researchers on the stack material, geometry and position within the resonator, focusing on numerical and experimental studies of standing wave thermoacoustic refrigerators [15-20]. Kajurek et al. [21] designed a mini refrigerator with 10 W cooling power and 30 °C temperature difference and used DeltaEC to

simulate their design. In the simulations, how the cold heat exchanger operates at different temperatures and different drive ratios is examined. Prashantha et al. [22] identified a strategy to develop thermoacoustic refrigerator design by using helium and air as working fluids. The result of the study showed that helium has a better cooling capacity than air and confirmed the theoretical results by comparing them with the DeltaEC simulation. Duman et al. [23] designed a 3 W laboratory-scale quarter wavelength TAR with a single stage and a spherical volume at the closed end and simulated this model with the DeltaEC program.

In this study, a thermoacoustic refrigerator using air as the working fluid with 12 W cooling power will be designed and the effects of operating frequency on viscous and thermal penetration depths, stack plate thickness and the gap between plates will be discussed. For this purpose, the optimization of the Taper, Small diameter tube and Divergent section with Hemispherical end resonator (TSDH) model, which is one of the resonator types used in the literature, will be done using the MATLAB program and the DELTA EC program will be used to check the validity of the results .

2. MATERIALS AND METHODS

2.1. Design Strategy of Standing Wave Thermoacoustic Refrigerator

In this chapter, the design process of a laboratory-scale thermoacoustic refrigerator with a cooling capacity of 12 W is explained step by step. The design steps discussed in this section can help researchers to design and manufacture compatible refrigerator models for home cooling that will replace traditional vapor compression refrigerators in the near future. The steps to be followed in the design of the components of a thermoacoustic refrigerator model are shown in Figure 1.

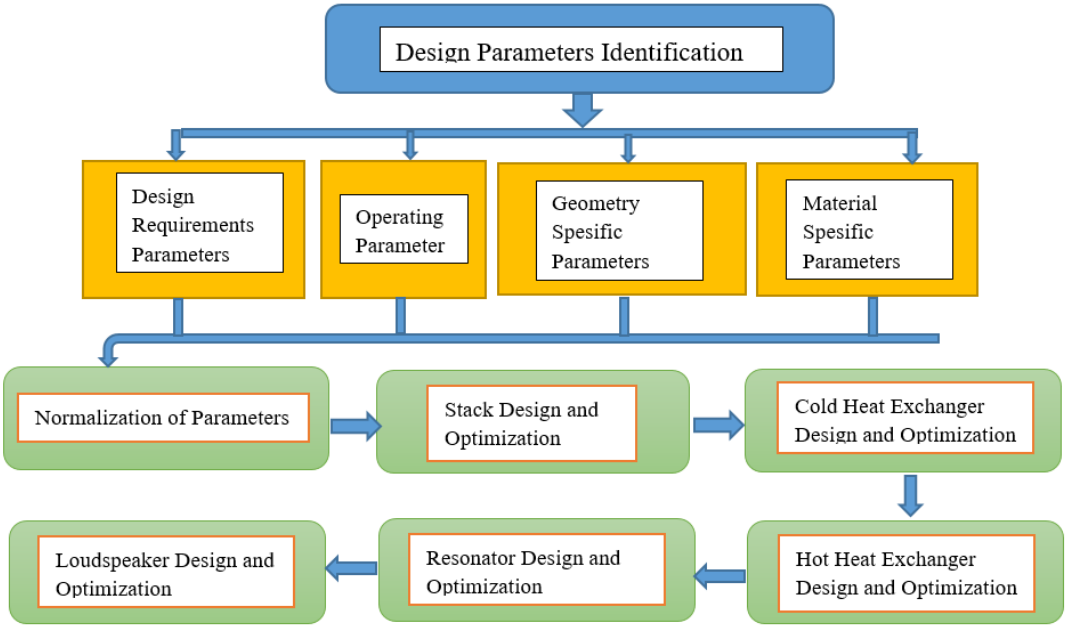

Figure 1. Design stages of standing wave Thermoacoustic refrigerator

The design of the thermoacoustic refrigerator starts with the defining design parameters step. All parameters used in the design are shown in table 1. The design and optimization of thermoacoustic refrigerators is difficult due to the large number of parameters. Therefore, as seen in Table 1, the number of independent parameters was reduced to 11 by applying the normalization technique to reduce the number of dependent parameters. These normalized individual parameters are used in the optimization and design of refrigerator components. The first component to start designing is the stack. The stack is used to pump heat from the cold heat exchanger to the hot heat exchanger and is considered the heart of the thermoacoustic refrigerator system. Optimization of the cooling effectiveness coefficient (COPy) of the stack is obtained by using the equations of normalized cooling power and acoustic power consumed in the stack [2,3,9,10].

$$Q = -\frac{1}{4}\Pi\delta_k\left(\frac{T_m\beta p_1^s\langle u_1^s\rangle}{(1+\varepsilon_s)(1+\sigma)\left(1-\frac{\delta_v}{y_0}+\frac{{\delta_v}^2}{2{y_0}^2}\right)}\right)x\left[\Gamma\frac{1+\sqrt{\sigma}+\sigma+\sigma\varepsilon_s}{1+\sqrt{\sigma}}-\left(1+\sqrt{\sigma}-\frac{\delta_v}{y_0}\right)\right]-\Pi(y_0K+lK_s)\frac{dT_m}{dx} \quad (1)$$

$$\dot{W} = -\frac{1}{4}\Pi\delta_k\Delta x\frac{(\gamma-1)\omega({p_1}^s)^2}{\rho_m a^2(1+\varepsilon_s)}x\left(\frac{\Gamma}{(1+\sigma)\left(1-\frac{\delta_v}{y_0}+\frac{{\delta_v}^2}{2{y_0}^2}\right)}-1\right)-\frac{1}{4}\Pi\delta_v\Delta x\frac{\omega\rho_m\langle{u_1}^s\rangle^2}{\left(1-\frac{\delta_v}{y_0}+\frac{{\delta_v}^2}{2{y_0}^2}\right)} \quad (2)$$

Considering the axial heat conduction effects, these equations have been non-dimensionalized and Equation (3) and Equation (4) have been obtained.

$$Q_{cn} = -\frac{\delta_{kn} D^2 sin(2x_n)}{8\gamma(1+\sigma)\Lambda}.\left[\frac{\Delta T_m\, tan(x_n)}{(\gamma-1)BL_{sn}}\frac{1+\sqrt{\sigma}\ +\sigma}{1+\sqrt{\sigma}} - \left(1+\sqrt{\sigma}-\sqrt{\sigma}\delta_{kn}\right)\right] - K_{pt}[B+(1-B)K^*]\Delta T_{mn}$$

$$\Lambda = 1-\sqrt{\sigma}\delta_{kn}+\frac{1}{2}\sigma{\delta_{kn}}^2,$$

$$K_{PT} = \frac{KT_m}{p_m \alpha L_S}, \qquad K^* = \frac{K_s}{K} \tag{3}$$

$$W_n = \frac{\delta_k L D^2}{4\gamma}(\gamma-1)Bcos(x_n)^2.\left(\frac{\Delta T_{mn}\tan(x_n)}{BL_{sn}(\gamma-1)\left(1+\sqrt{\sigma}\right)\Lambda}-1\right) - \frac{\delta_{kn}L_{sn}D^2}{4\gamma}\frac{\sqrt{\sigma}\sin(x_n)^2}{B\Lambda} \tag{4}$$

In this case, the cooling effectiveness coefficient (COPy) of the stack is as follows:

$$COP_y = \frac{Q_{cn}}{W_n} \tag{5}$$

According to the Carnot cycle, COPC is the theoretical cooling capacity of the refrigerant at a certain temperature difference and equation. It is indicated by (6).

$$COP_C = \frac{T_C}{T_H - T_C} \tag{6}$$

The coefficient of performance according to Carnot (COP_R) is defined as the ratio of the COP of the refrigerant to the COP of the Carnot cycle (COP_C) and is specified by equation (7).

$$COP_R = \frac{COP}{COP_C} \tag{7}$$

Stack length, stack center position and work consumed in the stack, stack cross-sectional area, stack diameter are obtained using the equations given in Table 1.

Table 1. Thermoacoustic refrigerator design parameters and normalized parameters

1.Design Requirement Parameters:
Cooling power (Q)
Desired temperature range (ΔT_x)
Total resonator volume (V_t)
Power density (P_v) of the resonator system
2. Working Parameters:
Resonator operating frequency (f)
Average gas pressure (P_m)
Dynamic pressure amplitude (P_a)
Working gas Average gas temperature (T_m)
Acoustic power input to resonator (W)
3. Geometry Specific Parameters:
3.1 Stack geometry
Space between stack plates ($2y_0$)
Stack plate thickness (2l)
Stack center position (X)
Stack length (l_3)
Stack cross section (A)
3.2 Resonator geometry
Resonator length (L_t)
4.Material Specific Parameters:
4.1 Stack material
density (ρ_s)
Stack thermal conductivity (K_s)
Stack specific heat (c_s)
4.2 Resonator material
Sound velocity (a)
Thermal conductivity of the working fluid (K)
Dynamic viscosity of the working fluid (μ)
Specific heats of the working fluid (c_p, c_v)
Density of the working fluid (ρ)
Wave number (k)
Thermal and viscous penetration depths (δ_k, δ_v)
Thermal expansion coefficient of the working fluid (β)
5.Normalized Parameter Optimization
Normalized stack length: $l_{3n} = kl_3$
Normalized stack center position: $X_{ns} = kX$
Normalized cooling power: $Q_{ns} = Q \div (P_m aA)$
Normalized acoustic power: $W_{ns} = W \div (P_m aA)$
Drive ratio: $D = P_m \div P_a$
Normalized temperature gradient: $\Delta T_{mn} = \Delta T \div T_m$
Porosity or Blockage rate: $B = y_0 \div (y_0+l)$
Normalized thermal penetration depth: $\delta_{kn} = \delta_k \div y_0$
Normalized viscous penetration depth: $\delta_{vn} = \delta_v \div y_0$
Prandtl number: σ
Specific heat ratio: γ

The second component to be designed is the cold and hot heat exchangers. The function of the cold heat exchanger (CHE) is to extract heat from the environment to be cooled and transfer it to the working fluid. The role of the hot heat exchanger (HHE) is to release the heat transferred by the stack in the CHE to the surrounding environment. The diameter of the heat exchangers (HHE and CHE) is the same as the diameter of the stack. Since the heat abandoned in the HHE will be approximately twice the heat absorbed in the CHE, the length of the HHE should be approximately twice the length of the CHE. Similar to the stack, the HHE and CHE lengths are obtained using the equations equation (8).

$$x_1 = \frac{p_1}{w\rho_m a} Sin(kx) \tag{8}$$

Another component to be designed, the TSDH quarter wavelength resonator model, is shown in Figure 2.

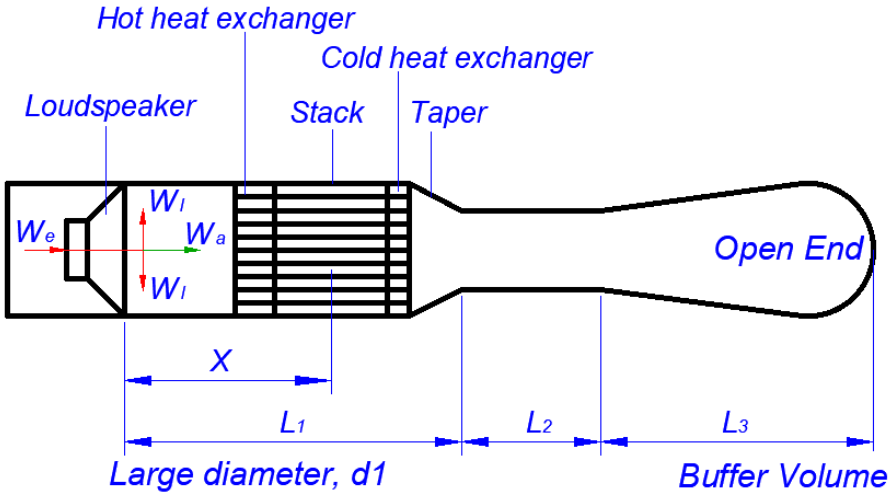

Figure 2. Quarter wavelength TSDH resonator model

The length of the resonator depends on the operating resonance frequency of the thermoacoustic system (usually a quarter or half wavelength) should be appropriate. The resonator must be perfectly isolated to prevent loss of acoustic power input. The last component to be designed is the speaker that provides the necessary acoustic power input for the thermoacoustic refrigerator system. Commercially available moving coil speakers have a much lower electro-acoustic efficiency of around 3-5%. However, the COP of the thermoacoustic refrigerator system mainly depends on the performance of the speaker. For effective COP, the speaker frequency must operate at the resonator frequency.

2.2. Design of 12 W Thermoacoustic Refrigerator Using Air as Working Fluid

In this section, a refrigerator with 12 W cooling power will be designed that uses air as the working fluid to create a 20 K temperature difference between the two ends of the stack. The parameters used in design calculations are given in Table 2.

Table 2. Parameters used in design

Design Parameters	Parameters of air as working fluid	Stack material Parameters
P_m= 100 kPa	a= 346.06 m/s	K_s = 0.155W/mK
T_m = 288 K	ρ_a = 1.169 kg/m ^{3}	ρ_s = 1353.6kg/ ^{m3}
ΔT= 20K	c_p = 1.0047kJ/kgK	c= 980.50J/kgK
f= 150Hz	c_v = 0.717 kJ/kgK	2l= 0.15mm
D= 0.04	Pr= 0.70738	$2y_0$ = 0.34mm
	K= 0.020608W/mK	

The average air temperature in the stack was chosen as 288 K. Thermal and viscous penetration depths δ_k, δ_v and Prandtl number (σ) used in the design of the stack were calculated with the equations given below.

$$\delta_k = \sqrt{\frac{K_a}{\rho_a c_{pa} \pi f}} \tag{9}$$

$$\delta_v = \sqrt{\frac{\mu_a}{\rho_a \pi f}} \tag{10}$$

$$\sigma_a = \left(\frac{\delta_v}{\delta_k}\right)^2 = \frac{\mu_a c_{pa}}{K_a} \tag{11}$$

The calculated δ_k and δ_v values with the operating frequency is given in Figure 3. As seen in the figure, it can be seen that as the operating frequency increases, the thermal and viscous penetration depths decrease.

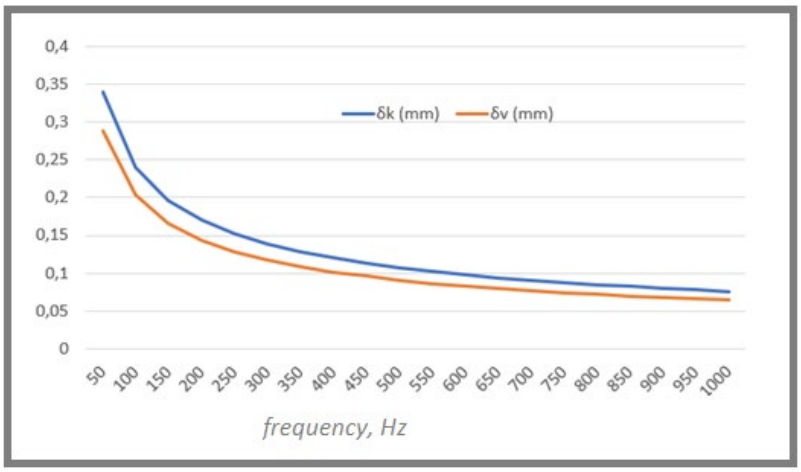

Figure 3. The variation of δk and δv values with the operating frequency

The porosity B (blockage ratio) of the stack is given by Eq. (12).

$$B = \frac{y_0}{(y_0 + l)} \tag{12}$$

Using the values given in Table 2 and Equation (12), the stack plate thickness (2l) is calculated as a function of the operating frequency at various values of the stack spacing in terms of thermal penetration depth (δ_k) and is given in Table 3. For parallel plate stack geometry, the optimal interplate spacing should be two to four times the thermal penetration depth [6]. As the operating frequency (f) increases, the stack plate spacing ($2y_0$) and thickness (2l) decrease. Additionally, as the value of the half-stack spacing (y_0), expressed in terms of thermal penetration depth δ_k, increases, the stack plate spacing (2y) and thickness (2l) also increase.

Table 3. Stack plate spacing and thickness versus frequency as a function of δ_k

f	$2y_0$ (mm)					2l (mm)				
Hz	δk	$1.25\delta_k$	$1.5\delta_k$	$1.75\delta_k$	$2\delta_k$	δk	$1.25\delta_k$	$1.5\delta_k$	$1.75\delta_k$	$2\delta_k$
50	0.680	0.850	1.020	1.190	1.360	0.120	0.150	0.180	0.210	0.240
100	0.481	0.601	0.721	0.841	0.962	0.085	0.106	0.127	0.148	0.170
150	0.393	0.491	0.589	0.687	0.785	0.069	0.087	0.104	0.121	0.139
200	0.340	0.425	0.510	0.595	0.680	0.060	0.075	0.090	0.105	0.120
250	0.304	0.380	0.456	0.532	0.608	0.054	0.067	0.080	0.094	0.107
300	0.278	0.347	0.416	0.486	0.555	0.049	0.061	0.073	0.086	0.098
350	0.257	0.321	0.386	0.450	0.514	0.045	0.057	0.068	0.079	0.091
400	0.240	0.301	0.361	0.421	0.481	0.042	0.053	0.064	0.074	0.085
450	0.227	0.283	0.340	0.397	0.453	0.040	0.050	0.060	0.070	0.080
500	0.215	0.269	0.323	0.376	0.430	0.038	0.047	0.057	0.066	0.076
550	0.205	0.256	0.308	0.359	0.410	0.036	0.045	0.054	0.063	0.072
600	0.196	0.245	0.294	0.344	0.393	0.035	0.043	0.052	0.061	0.069
650	0.189	0.236	0.283	0.330	0.377	0.033	0.042	0.050	0.058	0.067
700	0.182	0.227	0.273	0.318	0.363	0.032	0.040	0.048	0.056	0.064

2.3. Analysis of TSDH Resonator Design with 12 W Cooling Power

A review of the literature indicates that the quarter-wavelength TSDH resonator design is more effective than other designs [5,12]. In this section, the quarter-wavelength TSDH resonator shown in Figure 4 is designed. Calculations are carried out for different values of X_n and L_{sn} using the MATLAB programme and the results are given in Table 4. The values X_n = 0.2 and L_{sn} = 0.2, where COP and Qns values are high and W values are low, were selected for the design.

Table 4. Normalized stack center position and length values depending on acoustic power loss and COP

X_n	L_{sn}	d_1 (mm)	l_1 (mm)	l_2 (mm)	l_3 (mm)	l_4 (mm)	W (W)	Q_{ns} x 10^-5 (W)	COP
0.1	0.1	161	11	6	35	3	5.378	0.180411	2.231
0.2	0.1	146	42	10	35	5	4.082	0.218601	2.940
0.3	0.1	273	73	14	35	7	15.021	0.062246	0.799
0.2	**0.2**	**105**	**23**	**12**	**70**	**6**	**5.341**	**0.425975**	**2.247**
0.3	0.2	97	53	16	70	8	5.265	0.490289	2.279
0.4	0.2	103	84	20	70	10	7.004	0.442142	1.713
0.5	0.2	128	115	24	70	12	13.411	0.283454	0.895
0.6	0.2	476	148	26	70	13	227.091	0.020550	0.053
0.2	0.3	97	4	14	104	7	7.389	0.495099	1.624
0.3	0.3	86	34	18	104	9	6.679	0.632970	1.797
0.4	0.3	83	65	22	104	11	7.456	0.683663	1.609
0.5	0.3	85	96	26	104	13	9.660	0.645157	1.242
0.6	0.3	95	129	28	104	14	14.619	0.518988	0.821
0.3	0.4	81	15	20	139	10	8.340	0.704311	1.439
0.4	0.4	76	46	24	139	12	8.823	0.804424	1.360
0.5	0.4	75	79	26	139	13	10.488	0.826009	1.144
0.6	0.4	78	109	30	139	15	13.678	0.768207	0.877
0.4	0.5	73	26	26	174	13	10.375	0.876880	1.157
0.5	0.5	71	59	28	174	14	11.871	0.934520	1.011
0.6	0.5	71	90	32	174	16	14.632	0.917739	0.820
0.4	0.6	71	9	26	209	13	11.996	0.925184	1.000
0.5	0.6	68	40	30	209	15	13.432	1.006.861	0.893
0.6	0.6	68	72	32	209	16	16.068	1.017.426	0.747

Table 5 shows the dimensions and COP values of the optimized TSDH resonator as a function of normalized stack length and center combination.

Table 5. Theoretical performance results of the optimized TSDH resonator as a function of normalized stack length and center combination

Xn	Lsn	L_1	L_3	L_4	R	Θ(°)	W_R (W)	W (W)	COP	COP_R
0.1	0.1	55	323	69	80	13.96	0.060	5.439	2.206	0.167
0.2	0.1	92	250	112	73	16.26	0.049	4.132	2.904	0.219
0.3	0.1	129	198	63	137	34.62	0.167	15.188	0.790	0.060
0.1	0.2	74	283	102	68	13.50	0.043	8.745	1.372	0.103
0.2	**0.2**	**111**	**221**	**143**	**52**	**13.30**	**0.026**	**5.367**	**2.236**	**0.168**
0.3	0.2	147	178	153	49	15.30	0.022	5.287	2.270	0.170
0.4	0.2	184	144	148	51	19.60	0.025	7.029	1.707	0.128
0.5	0.2	221	118	124	64	28.49	0.038	13.449	0.892	0.067
0.1	0.3	92	250	120	65	14.57	0.039	12.420	0.966	0.072
0.2	0.3	129	198	152	48	13.75	0.022	7.411	1.619	0.121
0.3	0.3	165	160	159	43	15.00	0.017	6.696	1.792	0.134
0.4	0.3	202	131	153	41	17.47	0.016	7.472	1.606	0.120
0.5	0.3	239	107	139	42	21.64	0.017	9.677	1.240	0.093
0.6	0.3	275	88	117	47	28.27	0.021	14.640	0.820	0.061
0.1	0.4	110	223	130	64	15.92	0.038	16.152	0.743	0.056
0.2	0.4	147	178	155	47	14.75	0.021	9.538	1.258	0.094
0.3	0.4	184	144	158	41	15.76	0.015	8.356	1.436	0.107
0.4	0.4	221	118	150	38	17.86	0.014	8.837	1.358	0.101
0.5	0.4	257	97	135	38	21.15	0.013	10.501	1.143	0.085
0.6	0.4	293	79	116	39	26.22	0.014	13.692	0.876	0.065
0.1	0.5	129	198	137	63	17.60	0.037	19.905	0.603	0.045
0.2	0.5	166	159	156	46	16.12	0.020	11.692	1.026	0.077
0.3	0.5	202	131	155	39	16.76	0.015	10.081	1.190	0.089
0.4	0.5	239	107	145	36	18.79	0.013	10.388	1.155	0.086
0.5	0.5	275	88	129	35	21.84	0.012	11.883	1.010	0.075
0.6	0.5	312	71	108	36	26.63	0.012	14.644	0.819	0.061
0.1	0.6	147	178	140	62	19.30	0.036	23.666	0.507	0.038
0.2	0.6	184	144	154	45	17.50	0.019	13.856	0.866	0.065
0.3	0.6	221	118	149	39	18.16	0.014	11.832	1.014	0.076
0.4	0.6	257	97	138	35	20.08	0.012	12.008	0.999	0.075
0.5	0.6	294	79	120	34	23.27	0.011	13.443	0.893	0.067
0.6	0.6	329	64	100	34	27.84	0.011	16.079	0.746	0.056

As a result of the short stack approach and checking the boundary layer assumptions, it is seen that the stack length is much smaller than the wavelength. This confirms the short stack approach (l_3= 0.07m, λ = a/f, 2.307 m). The distance between the speaker and the hot heat exchanger (l_1) is 23 mm. The length of the hot heat exchanger (l_2) is 12 mm, the stack length (l_3) is 70 mm, and the length of the cold heat exchanger (l_4) is 6 mm. The length of the taper (l_5) is 20 mm. The length of the small diameter pipe (l_6 or L_2) is 221 mm. The radius R of the hemisphere is 52 mm. Stack and heat exchanger plate spacings ($2y_0$) and thicknesses (2l) are calculated as 0.34 mm and 0.12 mm, respectively. To obtain better performance when air is used as the working fluid, the diameter ratio (d_2/d_1) is taken as 0.54. A small divergence angle (θ) of 13.9° is provided in the throat section to avoid eddies and turbulence in the divergent section. The length of the divergent part was found to be 143 mm and therefore the total length of the resonator system was 547 mm. Hemisphere area (A_{hs}) and volume (V_{hs}) were found to be 0.017649 m^2 and 0.0003181 m^3, respectively .

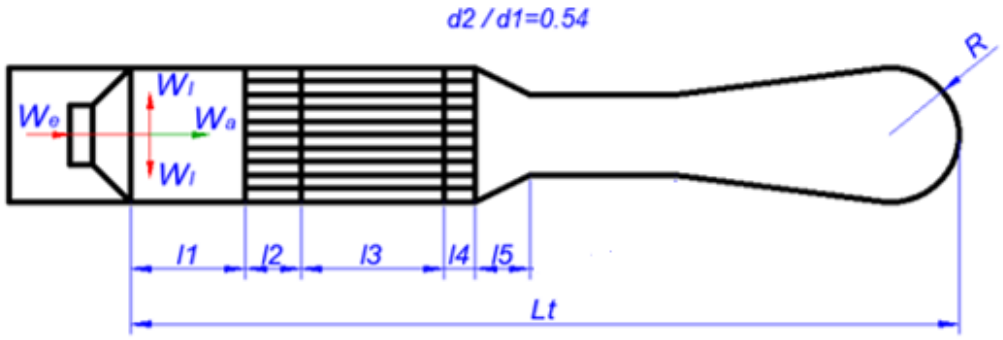

Figure 4. TSDH resonator design

3. RESULTS AND DISCUSSION

In this section, DeltaEC computer program was used to simulate the optimized TAR. DeltaEC computer program solves the one-dimensional wave equation in consecutive sections such as pipes, conical fittings, heat exchangers and stacks, whose geometry is given by the user, using a low-amplitude acoustic approach. Using the target estimation method, DeltaEC predicts and adjusts the initial unknown boundary conditions to achieve the desired boundary conditions at any location. In the simulation, the initial temperature, the phase angle of the pressure amplitude, the voltage of the acoustic driver, the heat abandoned from the hot heat exchanger and the gaps between the stack plates are the estimation Parameters. The real and imaginary parts of the normalized specific impedance, the calculated total energy flow at the end of the resonator, the cold and hot heat exchanger temperatures, and the phase difference between the pressure and volumetric flow amplitudes of the acoustic driver were selected as target parameters. The speaker values used in the DeltaEC simulation are given in Table 6.

Table 6. Electromechanical parameters of the speaker

Speaker Area	$A_p = 8.83.10^{-3}$ m^2
Electrical Resistance	$R_e = 4\ \Omega$
Mechanical Resistance	$R_m = 3$ Nsm^{-1}
Electrical Impedance	$L_e = 0.0013$ H
Moving Mass	m= 9.2 g
Force Factor	BL= 12.8 Tm
Spring Constant	s= 0 Nm^{-1}

Figure 5 shows the schematic picture of the designed TAR DeltaEC model.

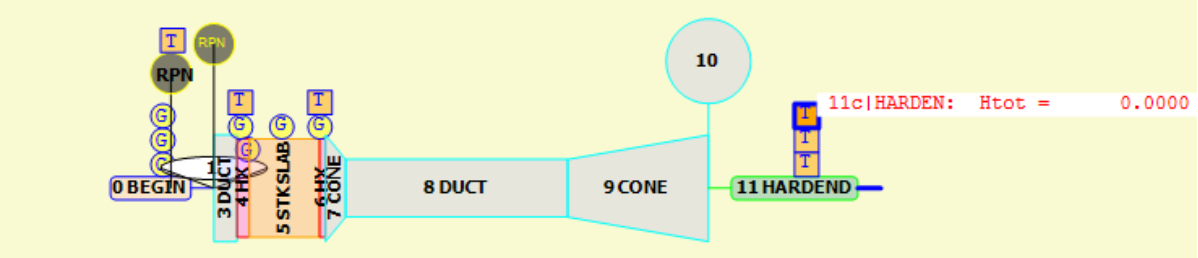

Figure 5. DeltaEC schematic representation of TAR

The results obtained from the DeltaEC simulation and the design results are given in Table 7.

Table 7. Design and DELTAEC Simulation results

Design results	**Simulation results**
f=150 Hz	f= 213.62 Hz
T=298K	T= 296.75 K
Q_c =12W	Q_c = 6.5481 W
W_T=5.367W	W_T= 7.2677 W
COP=2.236	COP = 1.036
COP_R = 0.168	COP_R = 0.075

As seen in Table 7, differences emerge between the design and simulation results. It is thought that these differences arise from not taking into account the speaker parameters and the damping effect in the conical parts during optimization.

The temperature difference chosen in the study is 20 K, which is 14.4 of the average temperature of the working fluid air, Tm = 288 K. Half of the gas gaps in the stack and heat exchanger system are taken as the same as the thermal and penetration layer depths. In the DeltaEC program, cold and hot heat exchanger temperatures are targeted as 278 and 298 K. Accordingly, the average temperature of the heat exchangers is 288 K. The refrigerator operates at 100 kPa pressure and 4% drive ratio. DeltaEC considers the entire resonator system, including the speaker, to be perfectly isolated. The hot heat exchanger releases to the surrounding environment an amount of energy equal to the sum of the cooling power of the cold heat exchanger and the electrical energy provided by the speaker. Figure 6 shows the variation of total power (E) depending on the x-axis. The total power (E) changes only at the x-axis positions where the heat exchangers and the stack are located along the length of the resonator, and there is no change in other parts. As seen in Figure 6, the total power takes the value of zero at the open end.

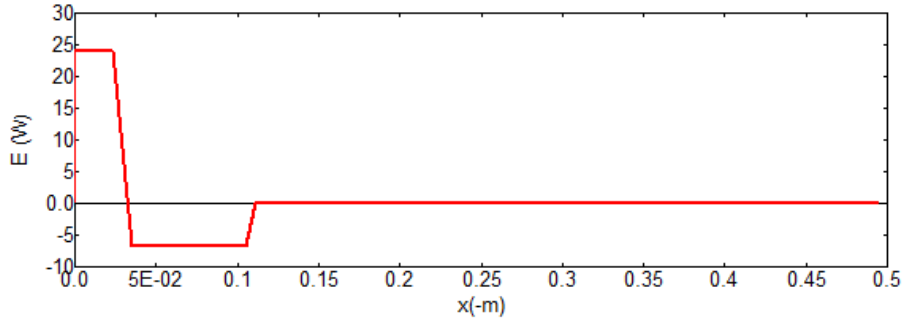

Figure 6. Variation of total power along the length of the resonator

Figure 7 shows the variation of acoustic power depending on the x-axis. As seen in the figure, acoustic power (W) decreases continuously along the positive x-axis. The biggest change in acoustic power occurs between the two ends of the stack and reaches zero at the open end of the device. The acoustic power absorbed in the stack is used to extract heat from the cooled environment.

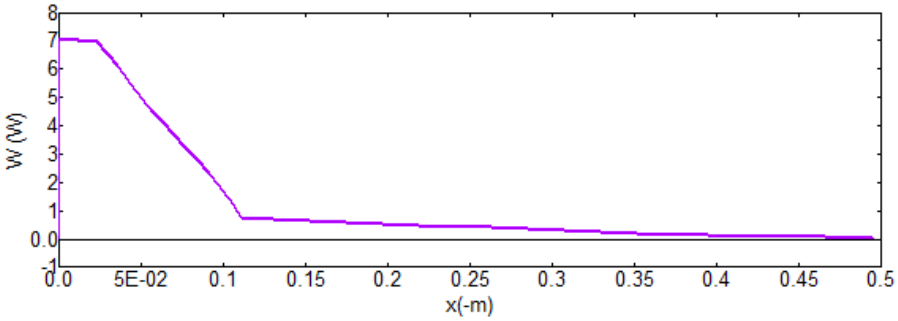

Figure 7. Variation of acoustic power along the length of resonator

Figure 8 shows the change of the operating fluid area along the x-axis. As seen in the figure, the working fluid area between the driver and the hot heat exchanger is one hundred percent and is equal to the cross-sectional area of the stack (A_p = 8.82 x 10^{-4} m^2). The working fluid area decreased significantly in the stack and heat exchangers, remained constant along the small diameter pipe, and then increased again in the tapered section.

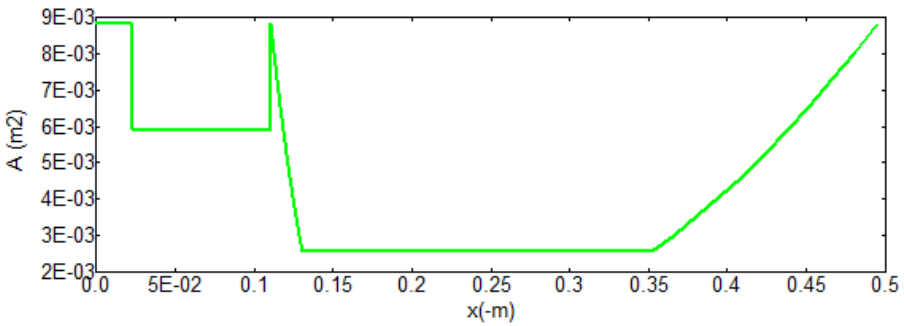

Figure 8. Gas field along the length of the resonator

Figure 9 shows the acoustic pressure amplitude variation along the x-axis. As seen in the figure, the acoustic pressure amplitude value is 4000 Pa in the driver position. This value remains constant until the heat exchanger and then decreases continuously along the x-axis.

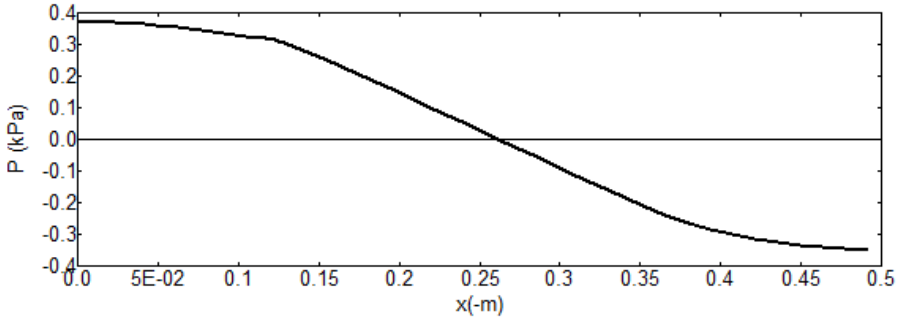

Figure 9. Acoustic pressure amplitude along the length of the resonator

Figure 10 shows the change of solid surface temperature (T_{Solid}) along the x-axis. As seen in the figure, the Tsolid temperature, which is 298 K at x = 0, shows a small decrease of approximately 3 K in the hot heat exchanger, and decreases significantly in the stack region and reaches 273 K in the cold heat exchanger. Since the resonator is considered to be perfectly insulated, it has been observed that the temperature in other parts does not change.

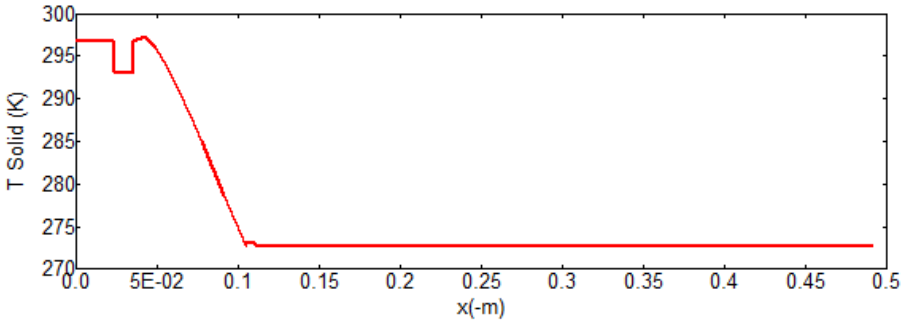

Figure 10. Solid surface temperature along the length of the TSDH resonator

Figure 11 shows the variation of the average temperature of the working fluid along the x-axis. As seen in the figure, the average surface temperature of the working fluid decreased significantly in the stack and did not change in the parts outside the stack.

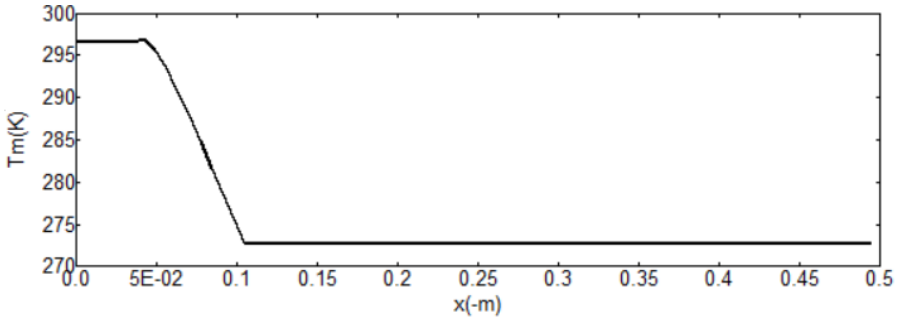

Figure 11. Average working fluid temperature along the length of the TSDH resonator

The change of TAR with cooling power at 288K average temperature, COP, is shown in Figure 12. As seen in the figure, as the cooling power increases, the COP increases and reaches its maximum value of 1.03 at 6.5 W of the cooling power.

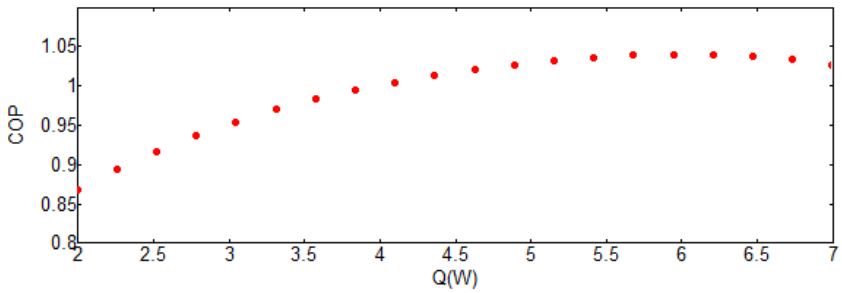

Figure 12. Variation of cooling power with COP

Figure 13 shows the change in COP_R with cooling power . As seen in the figure, as the cooling power increases, COP_R increases and reaches its maximum value of 0.075 at 6.5 W of the cooling power.

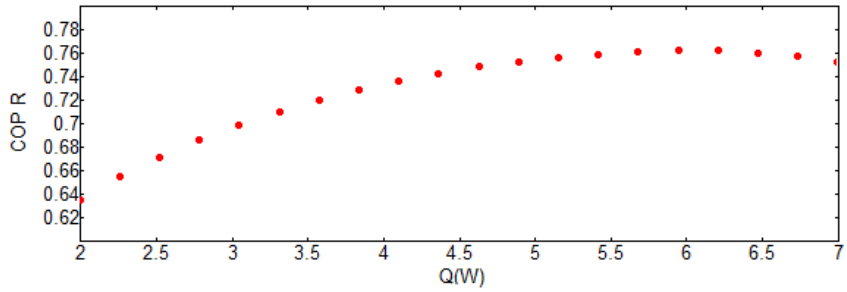

Figure 13. Variation of cooling power with COP_R

4. CONCLUSION

In this study, TSDH resonator design and simulation were carried out. The method to be followed in the design of the standing wave thermoacoustic refrigerator is explained step by step. The laboratory-scale TAR design with 12 W cooling power and TSDH geometry was made using the MATLAB program, and the validity of the obtained design values was investigated by entering them into the DeltaEC simulation program. In the simulation, it was assumed that the hot heat exchanger temperature was kept constant at 20 °C by using cooling water. The theoretical design and DeltaEC results are compatible with each other. However, theoretical results show a better performance than DeltaEC results. Because it seems that in the theoretical design, the speaker parameters and the damping effect in the conical part of the resonator after the cold heat exchanger are neglected. The optimization techniques discussed in this study aimed to improve the performance and cooling power of TAR. Experimental studies are needed to confirm the results obtained in this study.

NOMENCLATURE

a	Sound velocity, m/s	T_C	Cold heat exchanger temperature,K
A	Vertical cross-sectional area of the stack, m ^{2}	T_H	Hot heat exchanger temperature, K
A_p	Speaker cross-sectional area, m ^{2}	T_m	Average gas temperature, K
A_{hs}	Hemisphere area, m ^{2}	T_1	Acoustic temperature amplitude
B	Stack fill rate	T_{solid}	Solid surface temperature, K
BL	Force Factor, Tm	u_1	Velocity amplitude, m/s
c_p	Specific heat at constant pressure, J/kgK	u_1^s	Positive real part of the velocity amplitude
c_{pa}	Isobaric specific heat of air, J/kgK	P_v	Power density, W/ m^3
D	drive ratio	**Q**	Cooling power, W
d_1	Large pipe diameter, mm	Q_{cn}	Normalized cooling power
d_2	Small pipe diameter, mm	R_e	Drive electrical resistance, Ω
E	Total power, W	R_m	Drive mechanical resistance, Ns/m
f	Resonator frequency, Hz	**s**	Spring constant, kN/m
K	Thermal conductivity, W/mK	V_{hs}	Hemisphere volume, m ^{3}
K_s	Thermal conductivity of stack, W/mK	$\dot{W}$	Acoustic power, W
k	Wave number, rad/m	W_n	Normalized acoustic power
l	Half of the stack plate thickness, mm	**X**	Stack center position,mm

l_1	Distance from speaker to hot heat exchanger, mm	Δx	Gas parcel length,mm
l_2	Hot heat exchanger length, mm	σ	Prandtl number
l_3	Length of stack, mm	λ	Wavelength, m
l_4	Cold heat exchanger length, mm	μ	Dynamic viscosity of the working fluid, kg/ms
l_5	Length of conical part, mm	μ_a	Dynamic viscosity of the air, kg/ms
L_t	Total resonator length, mm	β	Coefficient of thermal expansion, K^{-1}
L_1	Length from driver to small diameter pipe, mm	δ_k	Thermal penetration depth, mm
L_2	Length of small diameter pipe, mm	δ_v	Viscous penetration depth, mm
L_3	Length of divergent part, mm	γ	Specific heat ratio
L_e	Driver input inductance, H	Γ	Normalized temperature difference
p_1	Pressure amplitude at a point, Pa	Λ	Air conduction correction factor
p_1^s	Positive real part of the pressure amplitude	Π	Perimeter length of stack and heat exchangers, mm
ρ	Density, kg/m^3	ω	Angular frequency
ρ_a	Density of air, kg/m^3	Θ	Parting angle, degrees
ρ_m	Average density, kg/m^3	ε_s	Ratio of fluid heat capacity to Stack material thermal capacity
TSDH	Taper, Small diameter tube and Divergent section with Hemispherical end resonator	COP	Cooling efficiency coefficient
CHE	Cold heat exchanger	COP_R	Coefficient of performance according to Carnot
HHE	Hot heat exchanger	COP_C	Carnot cooling effect coefficient

DECLARATION OF ETHICAL STANDARDS

The authors of the paper submitted declare that nothing which is necessary for achieving the paper requires ethical committee and/or legal-special permissions.

CONTRIBUTION OF THE AUTHORS

All authors contributed to the design and implementation of the research, to the analysis of the results and to the writing of the manuscript.

CONFLICT OF INTEREST

There is no conflict of interest in this study.

REFERENCES

[1] Alamir MA, Azwadi N. Thermoacoustic refrigerators and heat pumps: New insights for a high performance. Journal of Advanced Research in Fluid Mechanics and Thermal Sciences 2021; 78(1): 146–156. https://doi. org/ 10. 37934/ arfmts. 78.1.

[2] Zolpakar NA, Mohd-Ghazali N, El-Fawal MH. Performance analysis of the standing wave thermoacoustic refrigerator: A review. Renewable and Sustainable Energy Reviews 2016; 54: 626–634. https://doi.org/10.1016/j.rser.2015.10.018

[3] Tartibu LK. A sustainable solution for refrigeration using thermo-acoustic technology (March 2016). IInternational Conference on the Domestic Use of Energy (DUE) 2016; 1–8. https://doi. org/10.1109/ DUE. 2016.7466714

[4] Keolian RM, Garrett SL, Garrett SL. Thermoacoustics: A unifying perspective for some engines and refrigerators, Second Edition. Acoustical Society of America Journal 201; 143(4): 2110-2110. https://doi.org/10.1121/1.5031020

[5] Prashantha BG, Govinde Gowda MS, Seetharamu S, Narasimham GSVL. Design construction and performance of 10 W thermoacoustic refrigerators. International Journal of Air Conditioning and Refrigeration 2017; 25(03): 1750023. https://doi.org/10.1142/S2010132517500237

[6] Rott N. Thermoacoustics. Advances in applied mechanics 1980; 20: 135-175.

[7] Swift GW. Analysis and performance of a large thermoacoustic engine. the Journal of the Acoustical Society of America 1992; 92(3): 1551-1563.

[8] Wheatley J, Hofler T, Swift GW, Migliori A. Understanding Some Simple Phenomenain Thermoacoustics with Applications to Acoustical Heat Engines Acoustical Society of America 1985; 74(1).

[9] Hofler TJ. Thermoacoustic refrigerator design and performance (Heat Engine, Resonator, Microphone) 1986. University of California, San Diego.

[10] Minner BL, Braun JE, Mongeau L. Optimizing the design of a thermoacoustic refrigerator. Proceedings of the international refrigeration and air conditioning conference 1996. 343.

[11] Reid RS, Swift GW. Experiments with a flow-through thermoacoustic refrigerator. The Journal of the Acoustical Society of America 2000; 108(6): 2835-2842.

[12] Tijani MEH, Zeegers JCH, De Waele ATAM. Construction and performance of a thermoacoustic refrigerator 2002; Cryogenics, 42(1): 59-66.

[13] Hariharan NM, Sivashanmugam P, Kasthurirengan S. Experimental investigation of a thermoacoustic refrigerator driven by a standing wave twin thermoacoustic prime mover. International Journal of Refrigeration 2013; 36(8): 2420-2425.

[14] Wetzel M, Herman C. Design optimization of thermoacoustic refrigerators. International Journal of Refrigeration 1997; 20(1): 3–21. https://doi.org/10.1016/S0140-7007(96)00064-3

[15] Alamir MA. Experimental study of the stack geometric parameters effect on the resonance frequency of a standing wave thermoacoustic refrigerator. International Journal of Green Energy 2019; 16(8): 639–651. https://doi.org/10.1080/15435075.2019.1602533

[16] Zolpakar NA, Mohd-Ghazali N. Comparison of a thermoacoustic refrigerator stack performance: Mylar spiral, celcor substrates and 3D printed stacks. International Journal of Air-Conditioning and Refrigeration 2019; 27(03): 1950021. https://doi.org/10.1142/S2010132519500214

[17] Yahya SG, Mao X, Jaworski AJ. Experimental investigation wave thermoacoustic refrigerators. International Journal of Refrigeration 2017; 75: 52–63. https:// doi. org/10. 1016/j. ijref rig.2017.01.013

[18] Alcock AC, Tartibu LK, Jen TC. Experimental investigation of ceramic substrates in standing wave thermoacoustic refrigerator. Procedia Manufacturing 2017; 7: 79–85. https://doi.org/10. 1016/j.promfg.2016.12.021

[19] Zolpakar AN, Mohd-Ghazali N, Ahmad R. Optimization of the stack unit in a thermoacoustic refrigerator. Heat Transfer Engineering 2017; 38(4): 431–437. https://doi. org/10.1080/ 01457 632. 2016.1195138

[20] Tartibu LK. Maximum cooling and maximum efficiency of thermoacoustic refrigerators. Heat and Mass Transfer 2016; 52(1): 95–102. https://doi. org/10.1007/s00231-015-1599-y

[21] Kajurek J, Rusowicz A, Grzebielec A. Design and simulation of a small capacity thermoacoustic refrigerator. SN Applied Sciences 2019; 1(6): 1–9. https://doi.org/10.1007/ s42452-019-0569-2

[22] Prashantha BG, Swamy DR, Soragaon B, Nanjundeswaraswamy TS. Design optimization and analysis of thermoacoustic refrigerators. Int. J. Air-Conditioning Refrig. 2020; 28(3): 2050020. https://doi.org/10.1142/S2010132520500200

[23] Duman N, Acar Hİ, Yıldırım G. Design and Simulation of Thermoacoustic Cooling System. 24th Thermal Science and Technology Congress (ULIBTK'23) with international participation 2023, Ankara, Türkiye.